

Strength of ship plates under combined loading

Weicheng Cui^{a,*}, Yongjun Wang^b, Preben Terndrup Pedersen^c

^a *School of Naval Architecture and Ocean Engineering, Shanghai Jiao Tong University,
1954 Hua Shan Road, Shanghai 200030, People's Republic of China*

^b *China Ship Scientific Research Center, P.O. Box 116, Wuxi, Jiangsu 214082, People's Republic of China*

^c *Department of Naval Architecture and Offshore Engineering, Technical University of Denmark,
Building 101E, DK-2800 Lyngby, Denmark*

Received 13 January 2000; received in revised form 19 February 2001; accepted 7 March 2001

Abstract

Strength of ship plates plays a significant role in the ultimate strength analysis of ship structures. In recent years several authors have proposed simplified analytical methods to calculate the ultimate strength of unstiffened plates. The majority of these investigations deal with plates subjected to longitudinal compression only. For real ship structural plating, the most general loading case is a combination of longitudinal stress, transverse stress, shear stress and lateral pressure. In this paper, the simplified analytical method is generalized to deal with such combined load cases. The obtained results indicate that the simplified analytical method is able to determine the ultimate strength of unstiffened plates with imperfections in the form of welding-induced residual stresses and geometric deflections subjected to combined loads. Comparisons with experimental results show that the procedure has sufficient accuracy for practical applications in design. © 2001 Elsevier Science Ltd. All rights reserved.

Keywords: Unstiffened plates; Ultimate strength; Elastic large deflection analysis; Rigid–plastic analysis; Transverse compression; Lateral pressure

1. Introduction

A ship structure can be regarded as an assemblage of continuous stiffened plates with equally spaced longitudinal stiffeners of approximately the same size. The main load component for the deck structure, the bottom structure and longitudinal bulkheads close to the deck and bottom is axial compression. Therefore, in standard

*Corresponding author. Tel.: +86-21-62932056; fax: +86-21-62933160.

E-mail address: wccui@mail.sjtu.edu.cn (W. Cui).

Nomenclature

| | |
|-----------------------|---|
| a | plate length |
| a_t | breadth of tensile residual stress in the x direction |
| A_{ij0} | component of initial deflection function |
| A_{kl} | component of total deflection function |
| b | plate width |
| b_t | breadth of tensile residual stress in the y direction |
| D | plate bending stiffness ($= Et^3/12(1 - \nu^2)$) |
| E | Young's modulus |
| F | Airy's stress function |
| I | number of half-waves in the plate length direction for initial deflection |
| J | number of half-waves in the plate width direction for initial deflection |
| K | maximum number of half-waves tried for determining the final total deflection in the plate length direction |
| L | maximum number of half-waves tried for determining the final total deflection in the plate width direction |
| p | lateral pressure |
| t | plate thickness |
| w | total deflection function |
| w_p | the deflection due to lateral pressure |
| w_0 | initial deflection function |
| $w_{0\max}$ | maximum value of initial deflection function |
| α | aspect ratio ($= a/b$) |
| β | plate slenderness ($= (b/t)\sqrt{\sigma_0/E}$) |
| γ | ratio of b to t |
| ν | Poisson's ratio |
| ξ | longitudinal normalized residual stress |
| η | transverse normalized residual stress |
| ζ | the angle of the hinge line I |
| ϕ_u | normalized ultimate strength of plate ($= \sigma_u/\sigma_0$) |
| ϕ_x | $-\sigma_{x\text{av}}/\sigma_0$ (positive value for compression) |
| $\phi_{y/x}$ | the ratio between the transverse and longitudinal in-plane stresses |
| ϕ_v | normalized value of pressure ($= pE/\sigma_0^2$) |
| ψ_{ij0} | normalized value of A_{ij0} ($= A_{ij0}/t$) |
| $\psi_{0\max}$ | normalized maximum value of initial deflection function ($= w_{0\max}/t$) |
| ψ_{kl} | normalized value of A_{kl} ($= A_{kl}/t$) |
| σ_0 | yield stress |
| σ_{rc} | compressive residual stress (as negative value) |
| σ_{rt} | tensile residual stress ($= \sigma_0$, as positive value) |
| σ_u | ultimate strengths of plate |
| $\sigma_{x\text{av}}$ | average axial stress in the x direction (negative value for compression) |
| $\sigma_{y\text{av}}$ | average axial stress in the y direction (negative value for compression) |

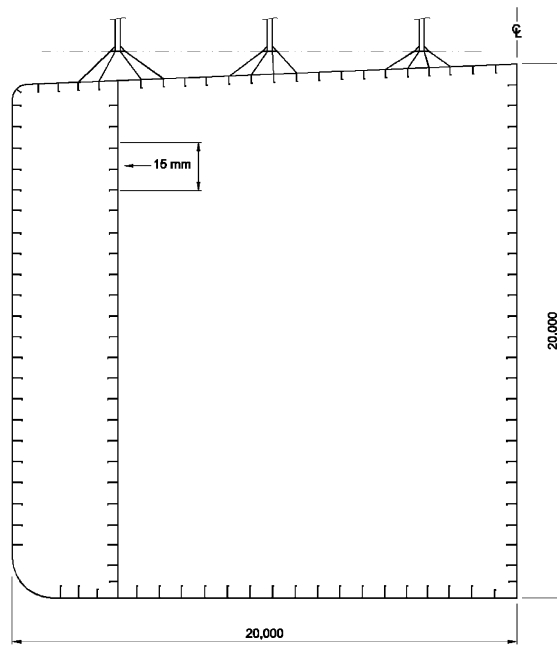


Fig. 1. A typical cross section of an FPSO.

design analyses of the ultimate hull girder bending moments, the only load components considered are longitudinal stresses. However, the external bottom plating and the lower parts of the side shells can in addition be subjected to relatively high external lateral pressure and the inner bottom and inner longitudinal bulkheads to lateral pressure loads from the cargo. These lateral pressures also either directly or through bending in web frames introduce transverse in-plane loads on the plate fields. As an example we can consider the relative magnitudes of the secondary stresses in the longitudinal bulkhead in a 100,000 DWT tanker converted into a floating production and storage facility (FPSO), see Fig. 1. A detailed linear finite element analysis of this tanker structure shows that the panels indicated by an arrow in Fig. 1 with dimensions $840 \times 4765 \times 15$ mm are subjected to in-plane stresses where the ratio between the transverse (vertical direction) and the longitudinal in-plane stresses equals $\sigma_y/\sigma_x = 0.45$. The source of these high compression stresses in the vertical direction is the weight of the production equipment arranged on the deck and outward bending of the wing tank. In addition, the plates are subjected to the tank pressure. It is obvious that for the design of the longitudinal bulkhead it is necessary to include the biaxial stress state of the plating in the analysis. It is also clear that the contribution to the longitudinal hull girder strength of these longitudinal bulkheads is reduced due to the secondary stresses. It is the purpose of the present paper to derive a design oriented procedure which can be used to quantify the ultimate strength of plates subjected to bi-axial compression in addition to lateral pressure.

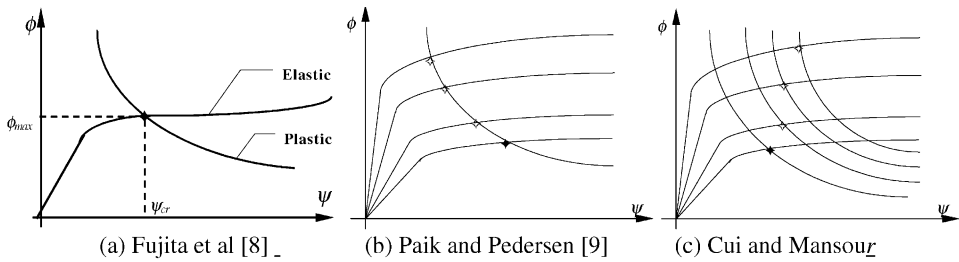


Fig. 2. Difference between procedures applied by Fujita et al. [8], Paik and Pedersen [9] and Cui and Mansour [10] to determine the ultimate strength.

The ultimate strength of ship plates is very important from the design and safety viewpoint because the collapse loads of plates can often act as an indicator of the ultimate strength of the whole stiffened panel in ship structures [1]. The problem has been addressed for centuries for the general plated structures and for several decades even with regard to ship structures [2,3]. The methods which have been proposed can be divided into: (1) finite element methods, (2) experiments, (3) empirical formulae which are based either on numerical or experimental results and (4) analytical or semi-analytical approaches. While most of the researches studied longitudinal compression only, some of them did consider the combined load cases, e.g. [4–7], but they used empirical approaches based on either FE or experimental results. In 1977 and 1979, a simplified analytical method was proposed by Fujita et al. [8] which combines the elastic large deflection theory and the rigid–plastic analysis based on admissible collapse mechanisms. In this method, the ultimate compressive strength is determined as the intersection value between the elastic and the rigid–plastic deflection solution, see Fig. 2a. However, if the shape of the initial deflection is complex, much computer time is still needed for the elastic large deflection analysis since a number of terms should be selected for describing the actual geometric configuration of the welding-induced initial imperfection [9].

In order to further reduce the computer time, Paik and Pedersen [9] made the assumption that the elastic large deflection analysis can be performed individually for each Fourier component of the deflection function. The ultimate compressive strength is then determined as the minimum intersection value among those estimated for individual components of the initial deflection function, see Fig. 2b.

In Ref. [9], it was assumed that for a given initial deflection component, the total deflection function always takes the same form as that of initial deflection component. In Ref. [10] Cui and Mansour argued that this may not always be the case, in particular when the amplitude of that initial deflection component is small. By removing this assumption, the simplified method was improved [10] (see Fig. 2c) and they further studied the effects of welding-induced residual stresses and the initial deflection shape and amplitude based on the simplified method [11].

However, all the above mentioned applications of the simplified analytically based method dealt with longitudinal stresses only. This loading condition is generally not

sufficiently representative for ship plating, as discussed above. Therefore, in this paper, the simplified analytical method developed in Refs. [9–11] is further generalized to deal with combinations of longitudinal stresses, transverse stresses and lateral pressure. Of course, in many situations shear stresses may also exist. However, shear stresses have not been considered in the present work.

2. Basic theory

The problem studied in this paper is a simply supported unstiffened plate subjected to a combination of longitudinal compressive stress, transverse compressive stress and lateral pressure, see Fig. 3. The basic approach adopted here is similar to that presented by Cui and Mansour in [10] but in the present paper a double Fourier series form is applied instead of single Fourier series for describing the welding-induced initial imperfection. Furthermore, the residual stresses in both the longitudinal and the transverse directions are considered.

2.1. Basic assumptions

The basic assumptions made in this development can be summarized as follows:

(1) The lateral pressure is assumed to be so small that small deflection theory can be applied to convert the lateral pressure into the deflection form. Although for the strength calculation the plate is assumed simply supported along all four sides, the

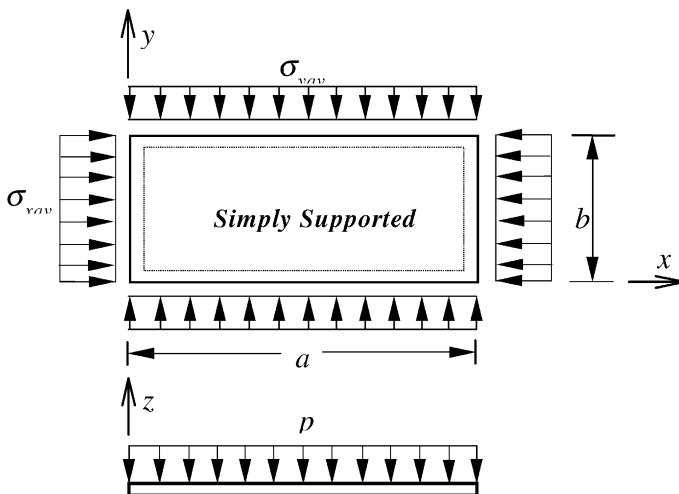


Fig. 3. A simply supported rectangular plate subjected to combined loading.

deflection induced by the lateral pressure alone will be close to the deflected shape of a clamped plate due to continuity across the stiffeners. Therefore, the following formula is used to approximate the deflection due to lateral pressure:

$$w_p = A_0 \left(1 - \cos \frac{2\pi x}{a} \right) \left(1 - \cos \frac{2\pi y}{b} \right). \quad (1)$$

Applying the energy method, the maximum deflection amplitude A_0 can be determined by

$$A_0 = \frac{pb^4}{Et^3} \frac{3(1 - \nu^2)}{\pi^4} \frac{\alpha^4}{(3\alpha^4 + 2\alpha^2 + 3)}, \quad (2)$$

where $\alpha = a/b$ is called the aspect ratio.

The deflection form given by Eq. (1) can be expanded into the following Fourier's series form:

$$w_p = t \sum_{i=1}^M \sum_{j=1}^N \psi_p(i, j) \sin \frac{i\pi x}{a} \sin \frac{j\pi y}{b}, \quad (3)$$

where $\Psi_p(i, j)$ is the normalized deflection component induced by lateral pressure. Here

$$\psi_p(i, j) = \frac{12\phi_v\beta^4}{ij\pi^6} (1 - \nu^2)(1 - \cos i\pi)(1 - \cos j\pi), \quad (4)$$

where

$$\beta = \frac{b}{t} \sqrt{\frac{\sigma_0}{E}} \quad \text{and} \quad \phi_v = \frac{pE}{\sigma_0^2}. \quad (5)$$

This deflection will be added to the initial deflection induced by welding. Due to the introduction of this simplification, the derived solution can only be applied to load cases with small lateral pressure. For plates in ship structures this is most often the case.

(2) The initial deflection configuration induced by welding and lateral pressure is approximated by the following Fourier series function:

$$w_0 = \sum_{i=1}^M \sum_{j=1}^N A_{ij0} \sin \frac{i\pi x}{a} \sin \frac{j\pi y}{b}, \quad (6)$$

where M and N will be selected depending on the complexity of the initial deflection shape.

(3) The elastic large deflection analysis and the rigid–plastic analysis are performed individually for each component of the deflection function. The interaction effects between deflection components are neglected.

(4) The initial deflection function with only one component from Eq. (6) is given as

$$w_0 = A_{ij0} \sin \frac{i\pi x}{a} \sin \frac{j\pi y}{b} \quad (7)$$

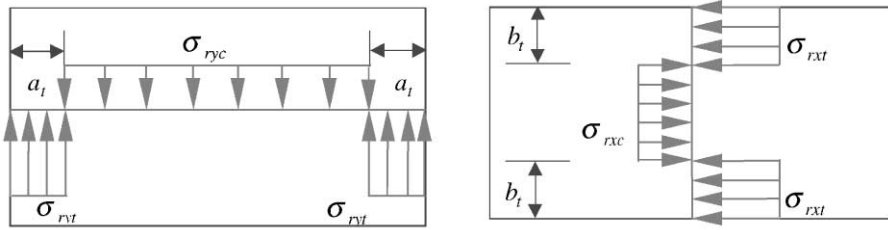


Fig. 4. Idealized welding-induced residual stress distribution.

and for this initial deflection function, the total deflection function is assumed to take the following form:

$$w = A_{kl} \sin \frac{k\pi x}{a} \sin \frac{l\pi y}{b}, \tag{8}$$

where k and l are determined by choosing the minimum intersection point. It may be worth to point out here that l is an integer in this paper rather than the distance it usually represents.

(5) The distributions of the residual stresses along the plate length and width are idealized as shown in Fig. 4:

$$\sigma_{ry} = \begin{cases} \sigma_{ryt}(= \sigma_0), & x \in (0, a_t), \\ \sigma_{ryc}, & x \in (a_t, a - a_t), \\ \sigma_{ryt}(= \sigma_0), & x \in (a - a_t, a), \end{cases} \tag{9}$$

$$\sigma_{rx} = \begin{cases} \sigma_{rxt}(= \sigma_0), & y \in (0, b_t), \\ \sigma_{rxc}, & y \in (b_t, b - b_t), \\ \sigma_{rxt}(= \sigma_0), & y \in (b - b_t, b), \end{cases} \tag{10}$$

where

$$a_t = \frac{a\eta}{2(1 + \eta)}, \quad \eta = -\frac{\sigma_{ryc}}{\sigma_0}, \tag{11}$$

$$b_t = \frac{b\xi}{2(1 + \xi)}, \quad \xi = -\frac{\sigma_{rxc}}{\sigma_0}. \tag{12}$$

(6) For the rigid–plastic deflection analysis, we consider two modes of kinematically admissible collapse mechanisms which depend on the aspect ratio.

(7) For each initial deflection component (i, j) , the deflection mode number (k, l) is to be determined by varying i from 1 to M and j from 1 to N and the set of (k, l) which has the lowest intersection value between the elastic large deflection solution and the rigid–plastic solution for the applied stress is chosen, see Fig. 2c. The number of modes M and N are subjectively chosen and generally $M = 11$ and $N = 3$ are adequate for practical applications. Then the ultimate strength of the plate is

determined as the minimum intersection value in the load–deflection plane among the response functions estimated for the individual components of the initial deflection function.

2.2. Elastic large deflection analysis

The general differential equation and the process of deriving the elastic large deflection solution are the same as in Ref. [10] and therefore these are omitted here. The Airy's stress function thus obtained is

$$\begin{aligned}
 F(x, y) = & \frac{Ea^2}{32b^2} \left[\frac{l^2}{k^2} \cos \frac{2k\pi x}{a} A_{kl}^2 - \frac{j^2}{i^2} \cos \frac{2i\pi x}{a} A_{ij0}^2 \right] \\
 & + \frac{Eb^2}{32a^2} \left[\frac{k^2}{l^2} \cos \frac{2l\pi y}{b} A_{kl}^2 - \frac{i^2}{j^2} \cos \frac{2j\pi y}{b} A_{ij0}^2 \right] \\
 & + \frac{1}{2} (\sigma_{x \text{ av}} + \sigma_{rx}) y^2 + \frac{1}{2} (\sigma_{y \text{ av}} + \sigma_{ry}) x^2.
 \end{aligned} \tag{13}$$

The final cubic equation can be written in the following form:

$$S\psi_{kl}^3 + P\psi_{kl} + Q = 0, \tag{14}$$

where all the parameters are expressed in non-dimensional form:

$$S = \frac{k^4}{16\alpha^2} + \frac{l^4\alpha^2}{16}, \tag{15}$$

$$\begin{aligned}
 P = & - \left(\frac{k^2 i^2 \delta_{lj}}{16\alpha^2} + \frac{l^2 j^2 \alpha^2 \delta_{ik}}{16} \right) \psi_{ij0}^2 + \frac{1}{12(1-v^2)} \left(\frac{k^2}{\alpha} + l^2 \alpha \right)^2 \\
 & - \frac{\phi_x \beta^2 k^2}{\pi^2} - \frac{\phi_{y/x} \phi_x \alpha^2 \beta^2 l^2}{\pi^2} - \frac{\alpha^2 \beta^2 l^2}{\pi^3 k} (1 + \eta) \sin \frac{k\pi\eta}{1 + \eta} \\
 & - \frac{\beta^2 k^2}{\pi^3 l} (1 + \xi) \sin \frac{l\pi\xi}{1 + \xi},
 \end{aligned} \tag{16}$$

$$Q = - \frac{1}{12(1-v^2)} \left(\frac{k^2}{\alpha} + l^2 \alpha^2 \right)^2 \psi_{ij0} \delta_{ik} \delta_{jl}, \tag{17}$$

where

$$\gamma = \frac{b}{t}, \quad \phi_{y/x} = \frac{\sigma_{y \text{ av}}}{\sigma_{x \text{ av}}}, \quad \psi_{ij0} = \frac{A_{ij0}}{t}, \quad \psi_{kl} = \frac{A_{kl}}{t}, \tag{18}$$

$$\phi_x = - \frac{\sigma_{x \text{ av}}}{\sigma_0}, \quad \phi_{y/x} = \frac{\sigma_{y \text{ av}}}{\sigma_{x \text{ av}}}. \tag{19}$$

When the initial deflection (including the lateral pressure) and residual stresses are zero, then Eq. (14) has positive roots only when $P < 0$. From this condition, a critical

value of β can be derived:

$$\beta_{\text{cr}} = \frac{(k^2 + l^2 \alpha^2) \pi}{2 \sqrt{3(1 - \nu^2) \alpha^2 (k^2 + \phi_{y/x} \alpha^2 l^2)}} \quad (20)$$

β_{cr} is the lowest value of β that the plate will fail by buckling. If the transverse stress is also zero, then β_{cr} is reduced to the von Karman constant [10]. Furthermore, for a given β and the condition that $P = 0$, we can also derive the critical buckling strength formula known from elastic small deflection theory:

$$\phi_{x \text{ cr}} = \frac{\pi^2 (k^2 + l^2 \alpha^2)^2}{12(1 - \nu^2) \alpha^2 \beta^2 (k^2 + \phi_{y/x} l^2 \alpha^2)} \quad (21)$$

2.3. Rigid–plastic solution

The general procedure for deriving the rigid–plastic solution is the same as in Ref. [10]. Assuming a possible collapse mechanism and by equating the internal energy W_I to the external work W_E , one can derive a rigid–plastic solution. The general expressions for the internal energy and the external work are as follows:

$$W_I = \sum_{n=1}^N \int_{l_n} M_{pn} \delta \theta_n \, dl_n, \quad (22)$$

$$W_E = \sum_{n=1}^N \int_{l_n} N_n w_n \delta \theta_n \, dl_n + W_p, \quad (23)$$

where W_p is the external work done by the lateral pressure, M_{pn} is the plastic bending moment per unit length along the hinge line, $\delta \theta_n$ is the change of the angle along the hinge line, N_n is the axial force per unit length along the hinge line and w_n is the deflection of the hinge line.

Two possible admissible collapse mechanisms are analyzed:

(1) $\alpha \geq k/l \tan \zeta$.

For this case, the collapse pattern is shown in Fig. 5. The geometrical conditions at collapse are

$$w_I = A_{kl} \left(1 - \frac{2l \sin \zeta}{b} l_n \right), \quad w_{II} = A_{kl},$$

$$\delta \theta_I = \frac{2l \delta A_{kl}}{b \cos \zeta}, \quad \delta \theta_{II} = \frac{4l \delta A_{kl}}{b}.$$

The axial force and the bending moment per unit length along the hinge lines I and II are calculated by

$$N_I = (\sigma_{x \text{ av}} \sin^2 \zeta + \sigma_{y \text{ av}} \cos^2 \zeta) t,$$

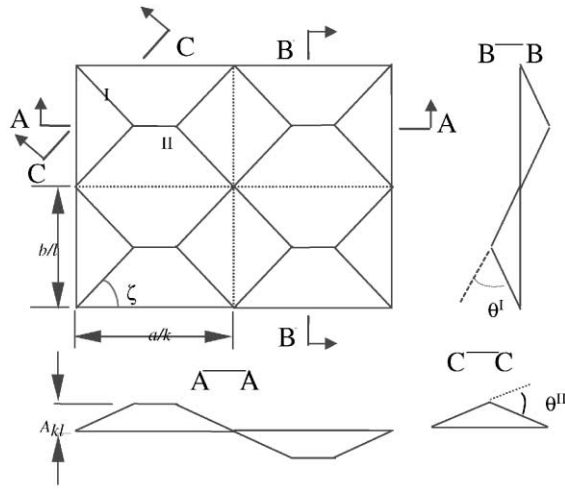


Fig. 5. The first assumed admissible collapse mechanism.

$$N_{II} = \sigma_{y \text{ av}} t,$$

$$M_p(\zeta) = m_p(\zeta) \frac{\sigma_0 t^2}{4}.$$

The expression for $m_p(\zeta)$ will be given later.

By substituting the above expressions for the geometric deflections and the force–deflection relations into Eqs. (22) and (23), we can obtain the following formulas for internal energy and the external work:

$$\begin{aligned} W_I &= 4 \int_0^{b/2l \sin \zeta} M_I \delta\theta_I dI_I + \int_0^{a/k - b/l \tan \zeta} M_{II} \delta\theta_{II} dI_{II} \\ &= \frac{M_I \delta A_{kl}}{2 \sin 2\zeta} + \frac{M_{II} \delta A_{kl}}{2} \left(\frac{al}{bk} - \frac{1}{\tan \zeta} \right), \end{aligned} \tag{24}$$

$$\begin{aligned} W_E &= 4 \int_0^{b/2l \sin \zeta} w_I N_I \delta\theta_I dI_{In} + \int_0^{a/k - b/l \tan \zeta} w_{II} N_{II} \delta\theta_{II} dI_{In} + W_p \\ &= 4 \frac{A_{kl}}{\sin 2\zeta} (\sigma_{x \text{ av}} \sin^2 \zeta + \sigma_{y \text{ av}} \cos^2 \zeta) \delta A_{kl} t \\ &\quad + 4 A_{kl} \left(\frac{al}{bk} - \frac{1}{\tan \zeta} \right) \sigma_{y \text{ av}} \delta A_{kl} t + W_p. \end{aligned} \tag{25}$$

The external work done by the lateral pressure is

$$W_p = \frac{pb}{6l} \left(\frac{3a}{k} - \frac{b}{l} \frac{1}{\tan \zeta} \right) \delta A_{kl}. \tag{26}$$

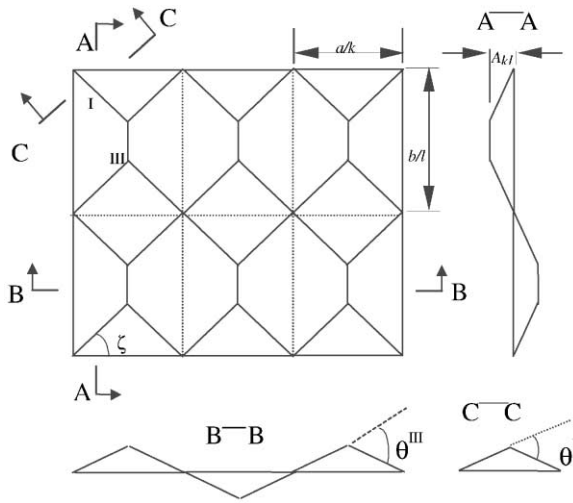


Fig. 6. The second assumed admissible collapse mechanism.

Using the upper bound theorem of plasticity $W_E = W_I$ and non-dimensionalizing the resulting expression we can derive the following rigid–plastic deflection solution:

$$R\psi_{kl} = T, \tag{27}$$

where

$$R = \frac{16}{\sin 2\zeta} (\phi_x \sin^2 \zeta + \phi_{y/x} \phi_x \cos^2 \zeta) + 16 \left(\frac{\alpha l}{k} - \frac{1}{\tan \zeta} \right) \phi_y, \tag{28}$$

$$T = \frac{m_I}{2 \sin 2\zeta} + \left(\frac{\alpha l}{k} - \frac{1}{\tan \zeta} \right) \frac{m_{III}}{2} - \frac{\beta^2 \phi_v}{6l} \left(\frac{3\alpha}{k} - \frac{1}{l \tan \zeta} \right). \tag{29}$$

$$(2) \alpha \leq k/l \tan \zeta.$$

For this case, the collapse pattern is shown in Fig. 6. The geometrical conditions at collapse are

$$w_I = A_{kl} \left(1 - \frac{2k \cos \zeta}{a} l_n \right), \quad w_{III} = A_{kl},$$

$$\delta\theta_I = \frac{2k \delta A_{kl}}{a \sin \zeta}, \quad \delta\theta_{III} = \frac{4k \delta A_{kl}}{a}.$$

The axial force and the bending moment along the hinge lines are given by

$$N_I = (\sigma_x \text{av} \sin^2 \zeta + \sigma_y \text{av} \cos^2 \zeta) t, \quad N_{III} = \sigma_x \text{av} t,$$

$$M_p(\zeta) = m_p(\zeta) \frac{\sigma_0 t^2}{4}.$$

By substituting these expressions into Eqs. (22) and (23), we can obtain the following formulas for internal energy and the external work:

$$\begin{aligned} W_I &= 4 \int_0^{a/2k \cos \zeta} M_I \delta \theta_I dl_I + \int_0^{b/l-a \tan \zeta/k} M_{III} \delta \theta_{III} dl_{III} \\ &= \frac{M_I \delta A_{kl}}{2 \sin 2\zeta} + \frac{M_{III} \delta A_{kl}}{2} \left(\frac{bk}{al} - \tan \zeta \right), \end{aligned} \quad (30)$$

$$\begin{aligned} W_E &= 4 \int_0^{a/2k \cos \zeta} w_I N_I \delta \theta_I dl_{In} + \int_0^{b/l-a \tan \zeta/k} w_{III} N_{III} \delta \theta_{III} dl_{III n} + W_p \\ &= 4 \frac{A_{kl}}{\sin 2\zeta} (\sigma_{x \text{ av}} \sin^2 \zeta + \sigma_{y \text{ av}} \cos^2 \zeta) \delta A_{kl} t \\ &\quad + 4 A_{kl} \left(\frac{bk}{al} - \tan \zeta \right) \sigma_{x \text{ av}} \delta A_{kl} t + W_p, \end{aligned} \quad (31)$$

$$W_p = \frac{pa}{6k} \left(\frac{3b}{l} - \frac{a}{k} \tan \zeta \right) \delta A_{kl}. \quad (32)$$

Using the condition $W_E = W_I$ and also non-dimensionalizing the expression we can derive the following rigid–plastic solution:

$$R\psi_{kl} = T, \quad (33)$$

where

$$R = \frac{16}{\sin 2\zeta} (\phi_x \sin^2 \zeta + \phi_{y/x} \phi_x \cos^2 \zeta) + 16 \left(\frac{k}{\alpha l} - \tan \zeta \right) \phi_x, \quad (34)$$

$$T = \frac{m_I}{2 \sin 2\zeta} + \left(\frac{k}{\alpha l} - \tan \zeta \right) \frac{m_{III}}{2} - \frac{\alpha \beta^2 \phi_v}{6k} \left(\frac{3}{l} - \frac{\alpha \tan \zeta}{k} \right). \quad (35)$$

(3) As the final step in the rigid–plastic collapse analysis, we need to calculate the plastic bending moment at collapse.

If we take a small element around the hinge line, its normal and shear stress distributions shown in Fig. 7 can be calculated from the following relations:

$$\sigma_1 = \sigma_{x \text{ av}} \sin^2 \zeta + \sigma_{y \text{ av}} \cos^2 \zeta,$$

$$\sigma_2 = \sigma_{x \text{ av}} \cos^2 \zeta + \sigma_{y \text{ av}} \sin^2 \zeta,$$

$$\tau = (\sigma_{x \text{ av}} - \sigma_{y \text{ av}}) \sin \zeta \cos \zeta.$$

Applying the von Mises yield criterion

$$\sigma_1^2 + \sigma_2^2 - \sigma_1 \sigma_2 + 3\tau^2 = \sigma_0^2,$$

$$\frac{\sigma_{1t}}{\sigma_{1c}} = \frac{\sigma_2 \pm \sqrt{4\sigma_0^2 - 12\tau^2 - 3\sigma_2^2}}{2},$$

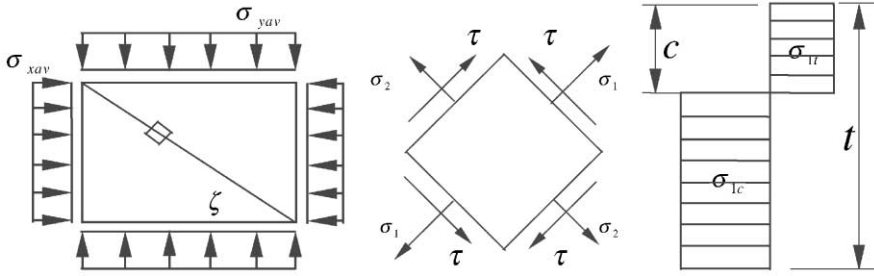


Fig. 7. Stresses in an element along the hinge line.

where σ_{1t} is the tensile yield stress and σ_{1c} is the compression yield stress along the hinge line

$$\sigma_{1t} = \sigma_{1t}c + \sigma_{1c}(t - c), \quad c = \frac{\sigma_1 - \sigma_{1c}}{\sigma_{1t} - \sigma_{1c}} t.$$

Thus the plastic bending moment for the hinge line is

$$\begin{aligned} M_p(\zeta) &= \sigma_{1t}c\left(t - \frac{c}{2}\right) + \sigma_{1c}\frac{(t - c)^2}{2} = m_p(\zeta)\frac{\sigma_0 t^2}{4} \\ &= \frac{t^2[\sigma_0^2 - (\sigma_{xav} + \sigma_{yav})^2 + \sigma_{xav}\sigma_{yav}]}{2\sqrt{4\sigma_0^2 - 3(\sigma_{sav} \sin^2 \zeta + \sigma_{yav} \cos^2 \zeta)^2 - 12(\sigma_{sav} - \sigma_{yav})^2 \sin^2 \zeta \cos^2 \zeta}}. \end{aligned} \tag{36}$$

From Eq. (36) we can obtain the following expression by further introducing the non-dimensional parameters:

$$m_p(\zeta) = \frac{2[1 - (\phi_x + \phi_{y/x}\phi_x)^2 + \phi_{y/x}\phi_x^2]}{\sqrt{4 - 3(\phi_x \sin^2 \zeta + \phi_{y/x}\phi_x \cos^2 \zeta)^2 - 12(\phi_x - \phi_{y/x}\phi_x)^2 \sin^2 \zeta \cos^2 \zeta}}. \tag{37}$$

For simplicity, the angle of ζ is taken to be 45° . In that case, the angles for hinge lines I, II and III are 45° , 0° and 90° , respectively.

By substituting the respective angles of ζ into Eq. (36), we can obtain the detailed expressions for m_I , m_{II} , m_{III} as follows:

$$m_I = m_p(45^\circ) = \frac{2[1 - (\phi_x + \phi_{y/x}\phi_x)^2 + \phi_{y/x}\phi_x^2]}{\sqrt{4 - 0.75(\phi_x + \phi_{y/x}\phi_x)^2 - 3(\phi_x - \phi_{y/x}\phi_x)^2}} \tag{38}$$

$$m_{II} = m_p(0^\circ) = \frac{2[1 - (\phi_x + \phi_{y/x}\phi_x)^2 + \phi_{y/x}\phi_x^2]}{\sqrt{4 - 3\phi_{y/x}^2\phi_x^2}} \tag{39}$$

$$m_{III} = m_p(90^\circ) = \frac{2[1 - (\phi_x + \phi_{y/x}\phi_x)^2 + \phi_{y/x}\phi_x^2]}{\sqrt{4 - 3\phi_x^2}} \quad (40)$$

3. Validation

The above procedures have been coded in a small Fortran code and validated through comparison with experimentally obtained collapse loads available in the literature.

As a first example we re-analyzed the 33 cases given in Ref. [9] and almost identical results have been obtained. This indicates that when the method degenerates to the case of only longitudinal compression, it gives the same results as those of [9,10].

The second example comes from Ref. [12] in which three plates have been tested in uniaxial compression. Since these plates are pin-jointed on the four sides, no residual stresses and initial deformation are considered. The results are shown in Table 1. Except for the second plate (No. 02), the agreement is very good. Furthermore, they are all on the conservative side. The reason for the large discrepancy in the second plate is that this plate has a large slenderness and in this case the collapse load is not easily identified.

As a third example we have chosen to analyze the 31 plates from SSC-276 [13], which have been tested in combined loading. The basic parameters are given in Table 2. Because the residual stresses and initial deflections were not given in this reference, we assume they are of average level and can be approximated by using existing empirical formulas.

Faulkner's formula [14] is used to approximate the longitudinal residual stress: $\xi = 2\delta/(\gamma - 2\delta)$. In general $\delta = 3-4.5$, while in this paper $\delta = 4$.

Cui and Mansour's formula [11] is used to calculate the initial deflection:

$$A_{i1} = w_{0\max} \frac{0.765}{i^{1.565}}, \text{ where } \frac{w_{0\max}}{t} = \begin{cases} 0.1\beta^2, & 1 \leq \beta \leq 2.5, \\ 0.25\beta, & 2.5 < \beta \leq 4. \end{cases}$$

Here, the effects of the transverse residual stresses and the initial deflection components for $j > 1$ on the ultimate strength are neglected.

For these 31 plates, we carried out a series of calculations using the combined loading and then compared the results with those of experiments. Although some

Table 1

A comparison of the predicted results with experiments for panels in Ref. [12]

| Panel | α | β | γ | σ_0 (MPa) | t (mm) | Exp. | Cal. | Exp./Cal. |
|--------|----------|---------|----------|------------------|----------|--------|--------|-----------|
| No. 01 | 0.6 | 2.9 | 71.463 | 330 | 12.44 | 0.6545 | 0.6451 | 1.0146 |
| No. 02 | 0.389 | 4.87 | 120 | 330 | 11.43 | 0.5545 | 0.4513 | 1.2287 |
| No. 03 | 1.743 | 2.61 | 61.8 | 358 | 14.17 | 0.7374 | 0.6808 | 1.0831 |

Table 2

Comparison of predicted results with experiments for panels with combined loads in Ref. [13] (average levels of residual stresses and initial deflections assumed)

| No. | α | β | $\phi_{y/x}$ | ϕ_v | Cal. | Exp. | Exp./Cal. |
|-----|----------|---------|--------------|----------|--------|--------|-----------|
| 1 | 3.0000 | 1.1000 | 0.0000 | 0.2000 | 0.9833 | 0.9340 | 0.9499 |
| 2 | 3.0000 | 1.1000 | 0.9790 | 0.0000 | 0.8148 | 0.5940 | 0.7290 |
| 3 | 3.0000 | 1.1000 | 0.3040 | 0.0000 | 1.0000 | 0.9820 | 0.9820 |
| 4 | 3.0000 | 1.8400 | 0.0000 | 0.2000 | 0.8734 | 0.7773 | 0.8900 |
| 5 | 3.0000 | 1.8400 | 0.2510 | 0.0000 | 0.8082 | 0.8060 | 0.9973 |
| 6 | 3.0000 | 1.8400 | 0.3830 | 0.0000 | 0.7119 | 0.6990 | 0.9819 |
| 7 | 3.0000 | 1.8400 | 0.8090 | 0.0000 | 0.4529 | 0.4306 | 0.9508 |
| 8 | 3.0000 | 1.8400 | 0.4750 | 0.0000 | 0.6534 | 0.5089 | 0.7788 |
| 9 | 3.0000 | 1.8400 | 0.5770 | 0.5660 | 0.3740 | 0.5204 | 1.3914 |
| 10 | 3.0000 | 2.5700 | 0.0000 | 0.2000 | 0.5761 | 0.5430 | 0.9425 |
| 11 | 3.0000 | 2.5700 | 0.7220 | 0.0000 | 0.3435 | 0.3900 | 1.1354 |
| 12 | 3.0000 | 2.5700 | 0.9580 | 0.0000 | 0.2720 | 0.2612 | 0.9603 |
| 13 | 3.0000 | 2.5700 | 0.5960 | 0.2050 | 0.2860 | 0.3930 | 1.3741 |
| 14 | 3.0000 | 2.5700 | 0.8960 | 0.1940 | 0.2112 | 0.2610 | 1.2358 |
| 15 | 3.0000 | 2.5700 | 0.8440 | 0.3020 | 0.1644 | 0.2610 | 1.5876 |
| 16 | 3.0000 | 3.3000 | 0.0000 | 0.2000 | 0.4049 | 0.4080 | 1.0077 |
| 17 | 3.0000 | 3.3000 | 0.0000 | 0.1980 | 0.4062 | 0.4110 | 1.0118 |
| 18 | 3.0000 | 3.3000 | 0.8020 | 0.2190 | 0.0905 | 0.2120 | 2.3425 |
| 19 | 3.0000 | 3.3000 | 0.8620 | 0.0000 | 0.2349 | 0.3188 | 1.3572 |
| 20 | 3.0000 | 3.3000 | 0.4680 | 0.2040 | 0.1605 | 0.4680 | 2.9159 |
| 21 | 3.0000 | 3.3000 | 0.7830 | 0.0000 | 0.2543 | 0.2130 | 0.8376 |
| 22 | 3.0000 | 3.3000 | 0.7960 | 0.2000 | 0.1108 | 0.2130 | 1.9224 |
| 23 | 3.0000 | 1.7400 | 0.8460 | 0.0450 | 0.4497 | 0.4065 | 0.9039 |
| 24 | 3.0000 | 1.7400 | 0.7650 | 0.0450 | 0.4881 | 0.4220 | 0.8646 |
| 25 | 3.0000 | 1.7400 | 0.0000 | 0.0900 | 0.8930 | 0.5895 | 0.6601 |
| 26 | 3.0000 | 4.0500 | 0.4980 | 0.0000 | 0.2818 | 0.2560 | 0.9084 |
| 27 | 3.0000 | 4.0500 | 0.5520 | 0.0300 | 0.2475 | 0.2270 | 0.9172 |
| 28 | 3.0000 | 4.0500 | 0.0000 | 0.0900 | 0.3328 | 0.3048 | 0.9159 |
| 29 | 3.0000 | 4.0500 | 0.1590 | 0.0000 | 0.3449 | 0.3826 | 1.1093 |
| 30 | 3.0000 | 4.0500 | 0.9370 | 0.0000 | 0.1819 | 0.1500 | 0.8246 |
| 31 | 3.0000 | 4.0500 | 0.3710 | 0.0000 | 0.3130 | 0.2547 | 0.8137 |

discrepancies exist, in general, they agree reasonably well, see Table 2. The reason for large discrepancies in some cases may be due to the approximation of residual stresses and initial deflections. What have been assumed here are the average level of the residual stresses and initial deflections and for some individual case, they could have large differences due to the scatter of the residual stresses and initial deflections. If the actual values of the residual stresses and initial deflections were available, the predictions could be improved. Therefore, the predictions are regarded as acceptable.

With all the different panels tested, it can be concluded that the method presented in this paper can provide reasonable predictions to the ultimate strength of unstiffened plates subjected to combined loading.

4. Discussion on various factors affecting the ultimate strength

The effects of aspect ratio, slenderness, initial deflection shape and amplitude, the residual stress along the width have been studied and they are found to be the same as that reported in Ref. [11], so these results will not be repeated here. The residual stress along the length has been found to have negligible influence on the ultimate strength, see Fig. 8. This indicates that for longitudinally dominated compression, the residual stresses induced by the welding in the transverse direction at the two ends are insignificant which confirms the neglect of these stresses in most of the methods. In this section, only those results which are unique to the present development are reported.

4.1. Effect of transverse stress on the longitudinal ultimate strength

In the present study, it is assumed that the longitudinal compression is the dominant applied load, so $\phi_{y/x}$ is less than 1. The effect of transverse compressive loads on the longitudinal ultimate strength is shown in Figs. 8 and 9. From Fig. 9 it can be seen that as the transverse stress increases, the longitudinal ultimate strength decreases almost linearly. Fig. 10 gives a comparison for the present prediction with the empirical formulas available in the literature [14–17]. It is seen that the agreement is reasonably good.

4.2. Effect of lateral pressure on the longitudinal ultimate strength

The effect of lateral pressure on the longitudinal ultimate strength is given in Fig. 11. It is seen that when the lateral pressure is small, it has a very small effect on the longitudinal ultimate strength.

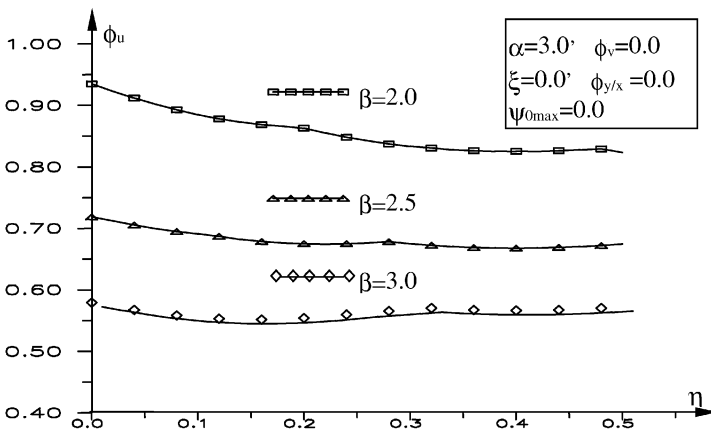


Fig. 8. Effect of transverse residual stress on the longitudinal ultimate strength.

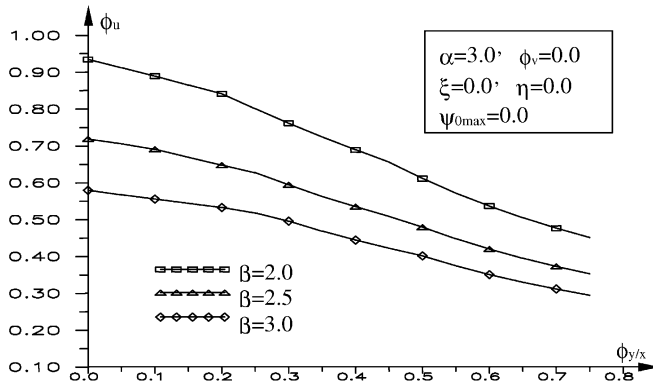


Fig. 9. Effect of transverse applied stress on the longitudinal ultimate strength.

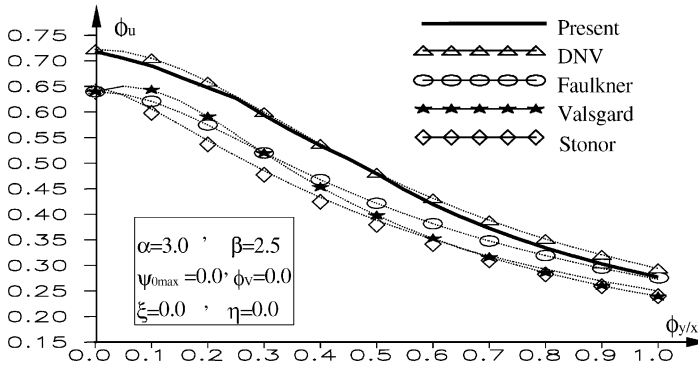


Fig. 10. A comparison of the present prediction with empirical formulas.

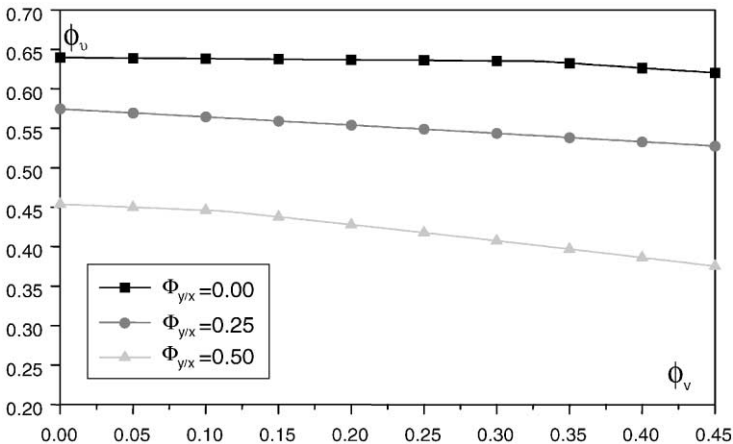


Fig. 11. Effect of lateral pressure on the longitudinal ultimate strength ($\alpha = 3.0, \beta = 2.5$).

5. Application of the present method in analysis and design

5.1. Derivation of the average stress–average strain curve

When applying Smith's approach for calculation of the ultimate strength of ship hulls [18,19], it is necessary to have average stress–average strain curves for plates and beam-columns. Using the solutions provided in this paper, the average stress–average strain curve for plates can be obtained.

From the elastic large deflection solution, we can obtain the following stress–strain relation:

$$\varepsilon = -\frac{\phi_x(1 - \nu\phi_{y/x})\beta^2}{\gamma^2} - \frac{\pi^2}{8\alpha^2\gamma^2}(k^2\psi_{kl}^2 - i^2\psi_{ij0}^2). \quad (41)$$

From the rigid–plastic solution, we can obtain the following stress–strain relations:

$$\varepsilon = -\frac{\phi_x(1 - \nu\phi_{y/x})\beta^2}{\gamma^2} - \frac{2kl\psi_{kl}^2}{\alpha\gamma^2}, \quad \alpha \geq k/l, \quad (42)$$

$$\varepsilon = -\frac{\phi_x(1 - \nu\phi_{y/x})\beta^2}{\gamma^2} - \frac{2k^2\psi_{kl}^2}{\alpha^2\gamma^2}, \quad \alpha < k/l. \quad (43)$$

Now if we define the average strain as

$$\bar{\varepsilon} = \frac{\varepsilon}{\varepsilon_0}, \quad \varepsilon_0 = -\frac{\sigma_0}{E} \quad (44)$$

and plot the elastic large deflection solution together with the rigid–plastic solution in the same figure, we can obtain the very familiar average stress–average strain curves used in the literature. Fig. 12 gives an example of these results. In comparing the present results with Fig. 6 of Ref. [20], the agreement is good except for the post-buckling behavior. Using this approach to derive the average stress–average strain relations, the effects of transverse stress and lateral pressure can also be taken into account.

5.2. Empirical design equations

For the convenience of applying the present results in design, a large set of parametric runs was carried out. Using curve fitting, the following empirical formulas have been derived for quick calculation:

$$\phi = \phi_b \delta_q \delta_c \delta_r \delta_a, \quad (45)$$

$$\phi_b = \begin{cases} 0.0614 + \frac{1.176}{\beta} + \frac{1.16}{\beta^2}, & \beta > 1.9, \\ 1.0, & \beta \leq 1.9, \end{cases} \quad (46)$$

$$\delta_q = 1 + 0.034\phi_v - 0.333\phi_v^2, \quad (47)$$

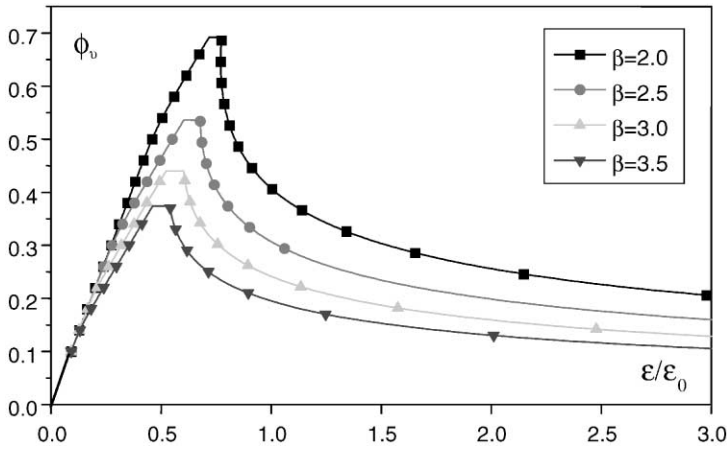


Fig. 12. Average stress–average strain derived from the present method ($\alpha = 3.0$, $\phi_{y/x} = 0.3$, $\phi_v = 0.2$).

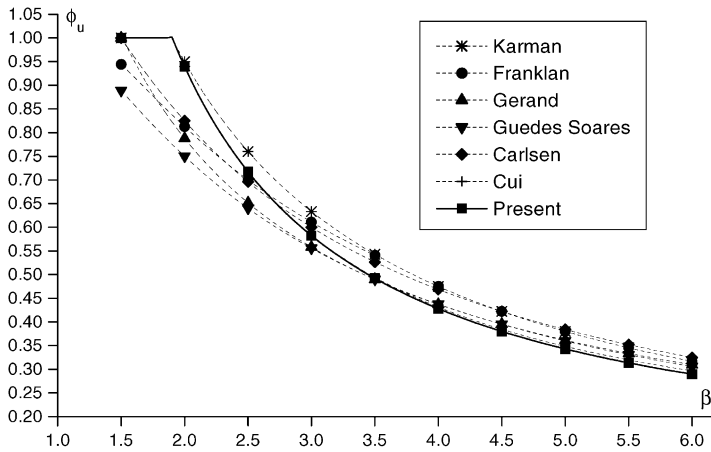


Fig. 13. A comparison of the present empirical formula with selected references.

$$\delta_c = 1 - 0.91\xi + 0.8244\xi^2 - 0.3077\xi^3, \tag{48}$$

$$\delta_r = 1 - 0.8155\phi_{y/x} + 0.1345\phi_{y/x}^2, \tag{49}$$

$$\delta_a = 0.9789. \tag{50}$$

For uniaxial compression Fig. 13 shows a comparison between this formula (Eq. (45)) and some other empirical expressions available in the literature (see Ref. [11]).

5.3. Interaction equation

Let us define

$$R_x = \frac{\phi_x}{\phi_{xu}} \quad \text{and} \quad R_y = \frac{\phi_{y/x}\phi_x}{\phi_{yu}}, \tag{51}$$

where ϕ_{xu} is the longitudinal ultimate strength when the transverse stress is not present. This value can be calculated by Eq. (45). The transverse compressive strength when the longitudinal stress is not present is ϕ_{yu} . This value can be approximated by the following formula [16]:

$$\phi_{yu} = \frac{\phi_{uF}}{\alpha} + 0.08 \left(1 + \frac{1}{\beta^2} \right)^2 \left(1 - \frac{1}{\alpha} \right), \tag{52}$$

where ϕ_{uF} is the ultimate strength formula given by Faulkner [21].

By curve-fitting the results calculated by the present procedure, the following approximation is obtained:

$$R_x^2 + 0.1135R_xR_y + R_y^2 = 1.0. \tag{53}$$

Fig. 14 shows the comparison of this equation with some other empirical formulas [14,15,17,22] and they also agree very well.

5.4. Ultimate strength analysis of plates in FPSO longitudinal bulkheads

As mentioned in Section 1, plates in FPSO longitudinal bulkheads have been found to be subjected to high level transverse stress together with lateral pressure. The present simplified analytical method is used to analyze their ultimate strength. The results are shown in Fig. 15. For this case, the effect of lateral pressure is quite significant because of the large aspect ratio.

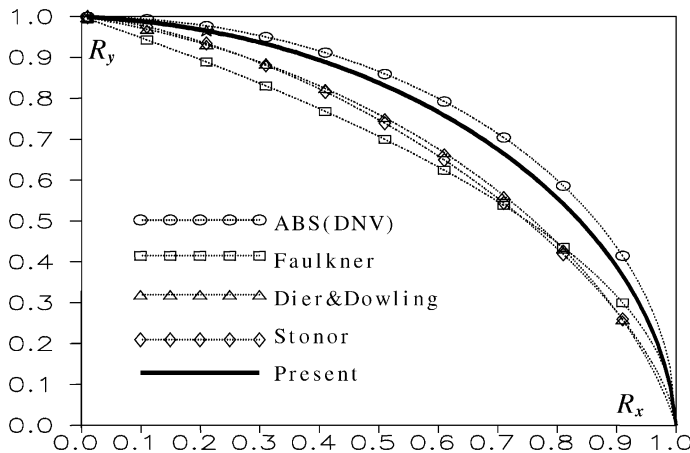


Fig. 14. A comparison of the predicted interaction equation with references.

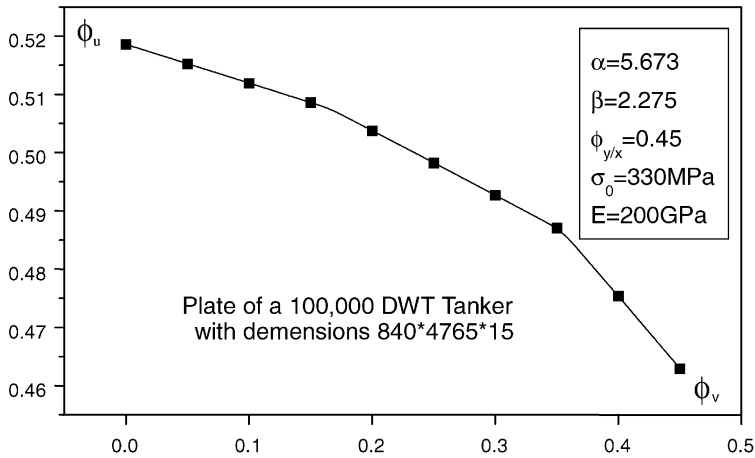


Fig. 15. Effect of lateral pressure on the longitudinal ultimate strength of plates in FPSO longitudinal bulkheads.

6. Summary and conclusions

The strength of ship plates is very important from the design and safety viewpoint. Although the problem has been addressed for long time, the solution to the problems is still not very satisfactory. Many methods have been proposed including (1) finite element method, (2) experiments, (3) empirical formulae which are based either on numerical or experimental results and (4) analytical or semi-analytical approaches. Among them the simplified analytical method proposed by Fujita et al. [8] has received a lot of attention recently. The method combines the elastic large deflection theory and the rigid–plastic analysis based on kinematically admissible collapse mechanisms. The advantage of this approach over the finite element method is that it is simple and efficient yet the results are reasonably accurate. The advantage over empirical formulas is that it is based on a rational theory and thus can bring more insight into understanding the nature of the structural behavior. Based on the previous successes [9–11], this paper further extends the method to deal with the situation where the plate is subjected to a combination of loads. Through this investigation, the following conclusions can be drawn:

- (1) The simplified analytical method is able to predict the ultimate strength of unstiffened plates under combined loading.
- (2) The effects of aspect ratio, slenderness and the residual stress distribution along the width are the same as those concluded in Ref. [11]. This further confirms the previous conclusion. However, the effect of the residual stress distribution along the length is found to be negligible.
- (3) The transverse compressive stress decreases the longitudinal ultimate strength in a reasonably linear way.

(4) Moderate lateral pressure has very small effect on the longitudinal ultimate strength. The prediction of this effect has also been compared with experimental results and they agree reasonably well.

(5) Using the present method, it has also been demonstrated that the average stress–average strain relation required in applying the Smith's method to predict the ultimate strength of ship hulls and the interaction relation between longitudinal stress, transverse stress and lateral pressure can be obtained. Furthermore, for the convenience of design application, an empirical formula is provided for quick estimation of the ultimate strength of plates under combined loading.

Acknowledgements

The paper is written during the first author's visit to Technical University of Denmark (DTU). Kind hospitality and financial support from Department of Naval Architecture and Offshore Engineering of DTU are greatly appreciated. Mr. Pei Junhou checked all the formulas presented in this paper and this is also acknowledged. Comments and additional references provided by one of the referees are appreciated. This research is supported by a project for fundamental researches for Chinese Shipbuilding Industry (project No. 99J40.3.5).

References

- [1] Guedes Soares C. Design equation for ship plate elements under uniaxial compression. *J Construct Steel Res* 1992;22:99–114.
- [2] Ueda Y, Tall L. Inelastic buckling of plates with residual stresses. *Publ Int Assoc Bridge Struct Eng* 1967;211–53.
- [3] Mansour AE. Post-buckling behaviour of stiffened plates with small initial curvature under combined loads. *Int Shipbuild Progr* 1971;18:1–71.
- [4] Steen E, Valsgard S. Simplified buckling strength criteria for plates subjected to biaxial compression and lateral pressure. *Ship Structure Symposium '84, SNAME*, 1984. p. 251–72.
- [5] Davidson PC, Chapman JC, Smith CS, Dowling PJ. The design of plate panels subjected to biaxial compression and lateral pressure. *Trans RINA* 1992;134:149–60.
- [6] Guedes Soares C, Gordo JM. Compressive strength of rectangular plates under biaxial load and the lateral pressure. *Thin-walled Struct* 1996;24:231–59.
- [7] Fujikubo M, Yao T, Khedmat MR. Estimation of ultimate strength of ship bottom plating under combined transverse thrust and lateral pressure. *J Soc Naval Archit Jpn* 1999;186:621–30.
- [8] Fujita Y, Nomoto T, Niho O. Ultimate strength of stiffened plates subjected to compression. *J Soc Naval Archit Jpn* 1977;141 (1st report); 1979;144 (2nd report) (in Japanese).
- [9] Paik JK, Pedersen PT. A simplified method for predicting ultimate compressive strength of ship panels. *Int Shipbuild Progr* 1996;43(434):139–57.
- [10] Cui WC, Mansour AE. Generalization of a simplified method for predicting ultimate compressive strength of ship panels. *Int Shipbuild Progr* 1999;46(447):291–303.
- [11] Cui WC, Mansour AE. Effects of welding distortions and residual stresses on the ultimate strength of long rectangular plates under uniaxial compression. *Mar Struct* 1998;11:251–69.
- [12] Max AMH. Simple design formulas for unstiffened and stiffened plates in uniaxial compression. Consulting Engineers, Aarau, Switzerland, 1971.

- [13] Becker H, Colao A. Compressive strength of ship hull girders. Part III: theory and additional experiments. SSC-276, 1977.
- [14] Faulkner D, Adamchak JC, Snyder JG, Vetler MF. Synthesis of welded grillages withstand compression and normal loads. *Comput Struct* 1973;3:221–46.
- [15] DNV. Buckling strength analysis. Classification note No. 30.1, Det norske Veritas, Hovik, Norway, 1992.
- [16] Valsgard S. Numerical design prediction of the capacity of plates in plate compression. *Comput Struct* 1980;12:729–39.
- [17] Stonor RWP, Bradfield CD, Moxham KE, Dwight JB. Tests on plates under biaxial compression. Report CVED/D-Struct/TR98, Cambridge University Engineering Department, 1983.
- [18] Smith CS. Influence of local compressive failure on ultimate longitudinal strength of a ship's hull. Practical design of ships and mobile units (PRADS), Tokyo, October 1977. p. 73–9.
- [19] Smith CS. Structural redundancy and damage tolerance in relation to ultimate ship hull strength. Proceedings of International Symposium on Role of Design, Inspection and Redundancy in Marine Structural Reliability, Williamsburg, VA, 1983.
- [20] Gordo JM, Guedes Soares C. Approximate load shortening curves for stiffened plates under uniaxial compression. In: Faulkner D, Cowling MJ, Incecik A, Das PK, editors. Integrity of offshore structures—5. EMAS, 1993. p. 189–211.
- [21] Faulkner D. A review of effective plating for use in the analysis of stiffened plating in bending and compression. *J Ship Res* 1975;19(1):1–17.
- [22] Dier AF, Dowling PJ. Plates under combined lateral loading and biaxial compression. CESLIC Report SP8, Department of Civil Engineering, Imperial College, London, 1980.